(Original Paper)

The Critical Growth Rate for Particle Incorporation during the Directional Solidification of Solar Silicon under Microgravity

Tina SORGENFREI [1], Thomas JAUSS [1], Arne CRÖLL [1],

Christian REIMANN [2], Jochen FRIEDRICH [2] and Martin VOLZ [3]

Abstract

   Foreign phase particles, which are engulfed by a growth front and then incorporated into a growing crystal, can cause a variety of problems. These problems can influence the crystal growth process and the preparation of the crystal or reduce the performance of resulting devices. In photovoltaics, the incorporation of SiC particles in VGF silicon leads to a relatively high material loss due to wire saw damages and shunts in the resulting solar cells. Due to the setup of the directional solidification the formation of SiC particles can hardly be avoided. Therefore, it is important to control the incorporation of the particles. It is known that the incorporation is dependent on the size of the particles and on the velocity of the moving solid-liquid interface. Existing theoretical models describe the transition between pushing and engulfment, but growth experiments show that the experimental values for the transition between these two states deviate significantly from the theoretical ones. In this work, several experiments under 1 G conditions and an experiment under µg conditions were done to investigate this question. The µg setup is necessary to get as close as possible to diffusive conditions which are the basic parameters for the theoretical calculations.

Keyword(s): Foreign phase particle, Particle engulfment, Particle pushing, Melt growth, Silicon, VGF, Directional solidification

Received 24 December 2015, Accepted 12 October 2016, Published 31 January 2017

1. Introduction

   The incorporation of foreign phase particles in growing bulk materials, independent of being single- or poly-crystalline is problematic for many applications. In photovoltaics this problem occurs during directional solidification of poly- and quasimono-crystalline silicon[1,2]. Due to the setup of the furnace and the environment during growth, certain amounts of nitrogen and carbon are dissolved in the Si melt. Once the melt is saturated and the melt volume decreases, solid silicon nitride (Si_3N_4) and silicon carbide (SiC) particles precipitate and move within the melt volume. The convection, influenced by thermal gradients, the size and design of the crucible, and external influences like rotating or travelling magnetic fields, define the movement of the particles. This movement leads sooner or later to the situation that the foreign phase particles get close or directly in contact with the growth front. Previous VGF experiments have shown that particles of bigger size are located near the bottom of the crucible, i.e. they were incorporated directly at the beginning of the growth, while smaller particles were incorporated at the end of the solidification process[3]. Thus

the growth velocity, and therefore the movement velocity of the solid-liquid interface, has a strong influence on what is happening with this particle in the moment when it is next to the interface. If a critical growth rate v_{cr} is achieved or exceeded, the particle will be engulfed by the growth front, below v_{cr} the particle will be pushed in front of the interface[4]. Thus, the incorporation of a particle depends on the growth velocity of the crystal. If a particle is engulfed and incorporated it will have a significant influence on the material performance. For example in solar silicon, hard SiC particles are responsible for a material loss due to sawing damages. The surface quality of the wafers is reduced because the wires of a wire saw may break or swing. Particles can also cause shunts in thin wafers, reducing material or device performance.

   Due to these problems it is necessary to either avoid the particle formation or -if that is not possible- to control the incorporation. There are many theoretical models trying to describe what is happening at the interface[5-11]. **Figure 1** describes the different forces acting on the particle in the melt in front of the solid-liquid interface. The first force is the so-called drag-force (F_D), it pushes the particle towards the interface. In

1   Crystallography, University of Freiburg, Hermann-Herder-Str. 5, 79104 Freiburg, Germany.
2   Fraunhofer Institute for Integrated Circuits and Devices, Schottkystr. 10, 91058 Erlangen, Germany.
3   NASA Marshall Space Flight Center, Huntsville, Alabama, USA.
(E-Mail : tina.sorgenfrei@fmf.uni-freiburg.de)

case of VGF and FZ, the second force, gravity (F_G) is working in the same direction, towards the interface. The third so-called lift-force (F_L), which originates from the convection driven melt movement parallel to the solid-liquid interface, and the interface force (F_I) are acting in the opposite direction.

Søiland[12] published a theoretical calculation of pushing/engulfment transitions in dependence of growth velocity and particle radius based on the formula of Stefanescu[13], which can be seen in **Fig. 2**. The common growth velocity for VGF-poly-Si is about 5.5 µm/s (= 0.33 mm/min). According to the calculation of Søiland the critical particle radius for engulfment should be around 1 mm. Particles with smaller radius should be pushed to the end of the crystal. Data from VGF experiments[1,2] show clearly that particles of much smaller sizes are already engulfed. This means that the model deviates significantly from the experimental data. There are a few points in which the model was simplified compared to the real experimental conditions: the interface roughness was neglected, the particles were assumed to be spherical, no chemical reaction or interaction of particle and melt were taken into account, and no melt convection (F_L=0) or gravitational segregation (F_G=0) were considered. To prove the theoretical model, experimental conditions close to the assumptions of the model are needed. The experiments have to provide a smooth solid-liquid interface, a certain range of defined and controllable growth velocities, diffusive and/or controlled convective conditions, and defined particles referring to chemistry, size, and shape, respectively. Except for diffusive conditions, all of the other assumptions can be realized and their degree of influence investigated on earth.

The suppression of convection can be achieved by very strong external static magnetic fields[14,15]. To prove this and investigate the particle behavior in this special case, experiments under static magnetic fields up to 5 Tesla were done at NASA Marshall Space Flight Center in Alabama, US. To reach diffusive conditions without any external field the tool of microgravity is necessary[9].

In this work several crystal growth experiments with different defined sizes of SiC particles in the silicon melt were done under 1 G and µg conditions to investigate the particle behavior in the growing material. For characterization after growth, different preparation and etching procedures were employed to determine the exact growth velocity at certain points. Infrared microscopy was used to find the exact positions of the incorporated particles and determine their size. With the knowledge of growth velocity, incorporation position, and particle size, respectively, v_{cr} can be calculated.

2. Experiments

2.1 Feed material Preparation and Growth

A growth technique with the possibility to control the growth direction is needed, because of a potential influence on the particle incorporation behavior of the crystal orientation. Furthermore, a precise control of the growth velocity is necessary. These requirements are compatible with the Float-Zone method (FZ). The FZ furnace used here is an ellipsoid

Fig. 1 Influencing, directional forces on a solid phase particle in a liquid or melt, F_D: drag-force of liquid melt, F_L: lift-force due to convectional melt movement with a certain velocity v_L, F_I: interface-force, F_G: gravitational force, v_{SL}: solid-liquid interface velocity[7].
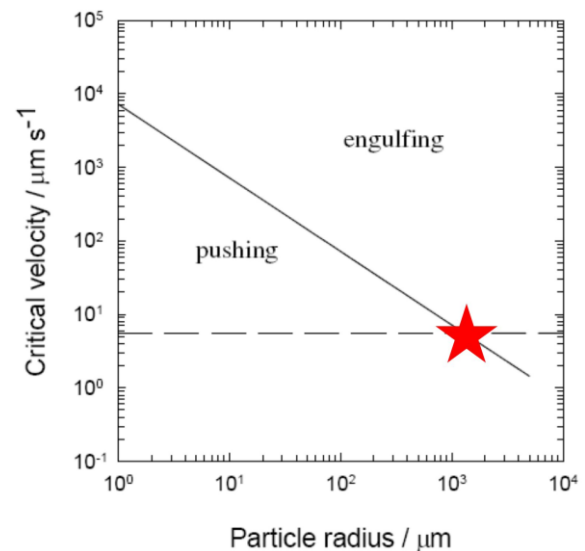
Fig. 2 Calculated transition between pushing or engulfing of particles in dependence of particle radius and the growth velocity[12]. The dashed line represents the typical growth velocity of 5.5 µm/s for the directional solidification of Si by VGF. The calculated critical particle radius for engulfment is given with ca. 1050 µm (red star).
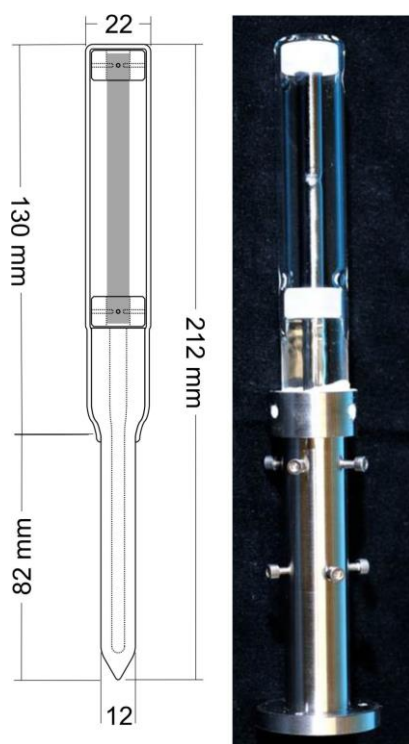
Fig. 3 Schematic sketch (left side) and picture (right side) of an ampoule used for growth experiments. The picture shows the filled fused silica ampoule fixed in the furnace holder, which can be mounted directly on the translation linkage (ready for experiment).

mirror furnace heated by halogen lamps[16]. This setup enables stable and high temperature gradients, which again allows a good control of the interface stability, shape, and movement. In FZ the growth direction can be controlled by using seeds of defined orientation.

On earth, the convection can be controlled or suppressed only within certain limits. While the gravity-driven buoyancy convection is always present on earth the surface tension-driven Marangoni convection can be avoided by avoiding free surfaces. This is realized by a silicon dioxide layer covering the whole crystal, produced before processing[17]. The silicon oxide does not melt at the melting temperature of silicon, so that a thin solid ductile skin of a few microns thickness covers the molten zone. The duration of contact between melt and skin in this experiment setup is about 5-10 minutes. The time is too short for dissolution of the oxide in the Si melt, and the evaporation of the oxide layer as SiO is avoided by an oxygen counter pressure in the sample environment.

To realize a convection free state within the melt, the buoyancy convection also has to be switched off. This can only happen in weightlessness or microgravity. In other words, diffusive conditions are created in an experiment under µg and without any free surfaces.

To investigate the critical growth velocities in dependence of the particle size, such a diffusive regime is needed to separate convectional influences from the velocity of interface movement.

In this work, different experiments with different particle sizes of SiC and different growth velocities were performed. For all experiments the same experimental setup was chosen. Rods of single crystalline, B-doped Czochralski grown Si with a diameter of 8 mm were prepared with an amount of 4 mg of SiC particles at the position of the first molten zone. The rods act as seed as well as feed material for the growth. The (001) orientation was chosen to define the growth direction [001] which forms no core facet, resulting in a smooth interface with slightly convex shape. The avoidance of a core facet was chosen to ensure homogenous properties and conditions at the interface without any discontinuity. In the presence of a core facet undercooling effects must also be considered. To investigate the influence of Marangoni convection on earth, experiments with and without oxide skin on the crystals were performed. An influence of the oxygen content dissolved from the oxide skin in the silicon can be excluded. The oxygen content was measured by FTIR for various samples and no influence of different oxygen contents was observable. If an oxide skin is used, the growth must happen in an oxygen atmosphere to ensure the stability of the skin during the whole growth duration. Therefore, the samples have to be put into an ampoule with a defined oxygen pressure. For comparability reasons the samples without oxygen skin were also processed in ampoules with an argon counter pressure. A schematic setup and a picture of the used ampoules are shown in **Fig. 3**. The ampoule material is fused silica. A base is needed for fixation of the sample to the translation mechanism within the mirror furnace. The crystal itself is held and centered by two fused silica rings and ceramic pins at the upper and the lower end of the rod.

Different translation velocities of the ampoule between 0.2 and 10 mm/min were applied and differently sized particles were used for the experiments. The d_{50} values of the classified SiC particles are 7 µm, 60 µm, 150 µm, and 300 µm, respectively.

2.2 µg Experiment

An experiment under microgravity is necessary to determine the strength of influence of the gravitational force. The experiment was performed during the TEXUS-51 mission in April 2015, launched from Esrange, Kiruna, Sweden. The TEXUS platform provides about 6 minutes of µg. During this time one growth experiment can be done. To receive the highest amount of information, in this experiment 2 sizes of SiC particles, 7 µm and 60 µm, were put into the rod and 3 different translation velocities, 2, 5 and 10 mm/min were applied. The sample setup was the same compared to the 1 G experiments and a mirror furnace identical in construction to the 1 G model was used.
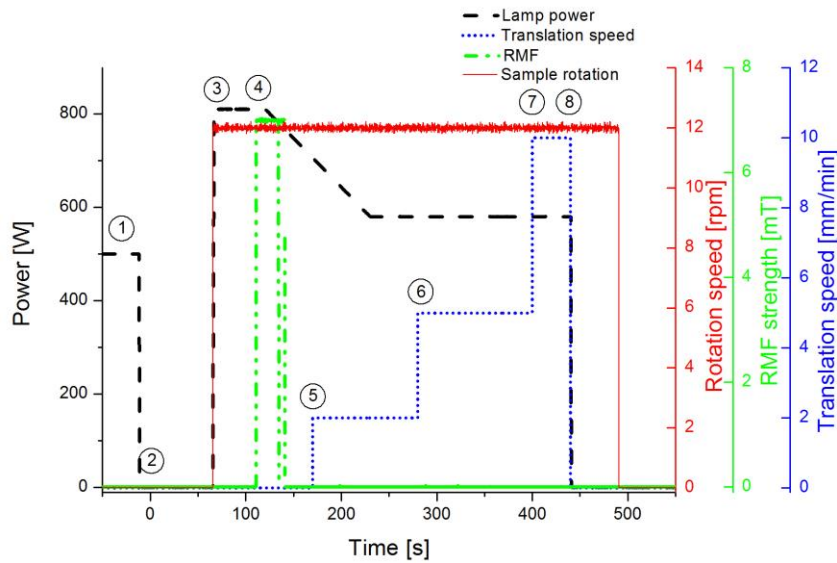
Fig. 4 Timeline (different growth parameters: black dashed line: lamp power in W, red solid line: sample rotation speed in rpm, green dashed-dotted line: RMF strength in mT, and blue dotted line: sample translation speed in mm/min) of growth experiments used in 1 G as well as in µg. Explanation to circled numbers: 1= pre-heating of sample before start to reduce melting time during flight, 2 = launch of rocket, 3= start of heating, 4= RMF is switched on for homogenization before crystal growth and after complete melting power is reduced to stabilize system, 5= start of crystal growth with translation speed of 2 mm/min, 6= increase of translation speed to 5 mm/min, 7= last experimental section with translation speed of 10 mm/min, 8= end of experiment.

3. Results

3.1 Pre-flight Experiments under 1 G

To obtain results from the 1 G experiments which are fully comparable to the µg experiment on TEXUS, a growth profile has to be used which can be established on both platforms. As mentioned above, TEXUS provides about 6 minutes of µg conditions which can be used for the experiment. Based on this limitation, a profile has to be applied which leads to a suitable length/volume of grown material for characterization. To achieve this and also to cover a big range of growth velocities during these 6 minutes, three different translation speeds were applied. The first translation speed of 2mm/min was held for 120 sec, then 5 mm/min for 120 sec, and at last 10 mm/min for 40 sec until the end of the experiment. The timeline is shown in **Fig. 4**. This timeline or parts of it were investigated in detail on earth to proof the reliability in µg. The resulting real growth velocity does not exactly equal the applied translation speed, thus a real growth velocity of 10 mm/min could not be achieved. As shown in **Fig. 4**, at the end of the growth experiment a steady increase of the growth velocity up to a maximum of 7-9 mm/min can be obtained. The results of the 1 G experiments are shown in **Fig. 5**. The blue solid line represents the theoretical transition between engulfing and pushing in dependence of the growth velocity and the particle diameter calculated by

Søiland[12]. The green points represent experimental data (particle size and growth velocity), where the particles were not incorporated into the growing crystal. The slugs did not disintegrate into single particles upon melting. Larger chunks and smaller chunks as well as a few single particles showed similar behavior, however, depending on the single particle size as can be seen in **Fig. 5**. Apparently, the critical velocity depends on the size of the single particles not on the aggregate
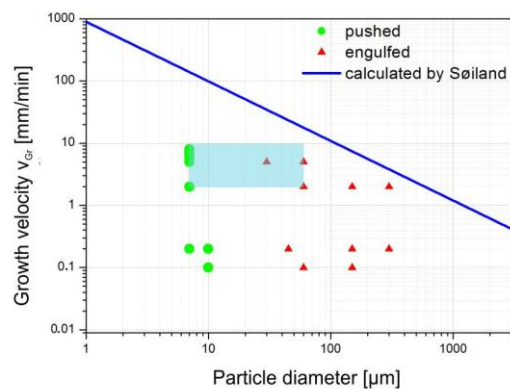
Fig. 5 Overview of 1 G experimental results: green points represent growth conditions and particles sizes pushed, red triangles represent engulfing conditions, and the blue line shows the theoretical transition between pushing and engulfing region calculated by Søiland[12].
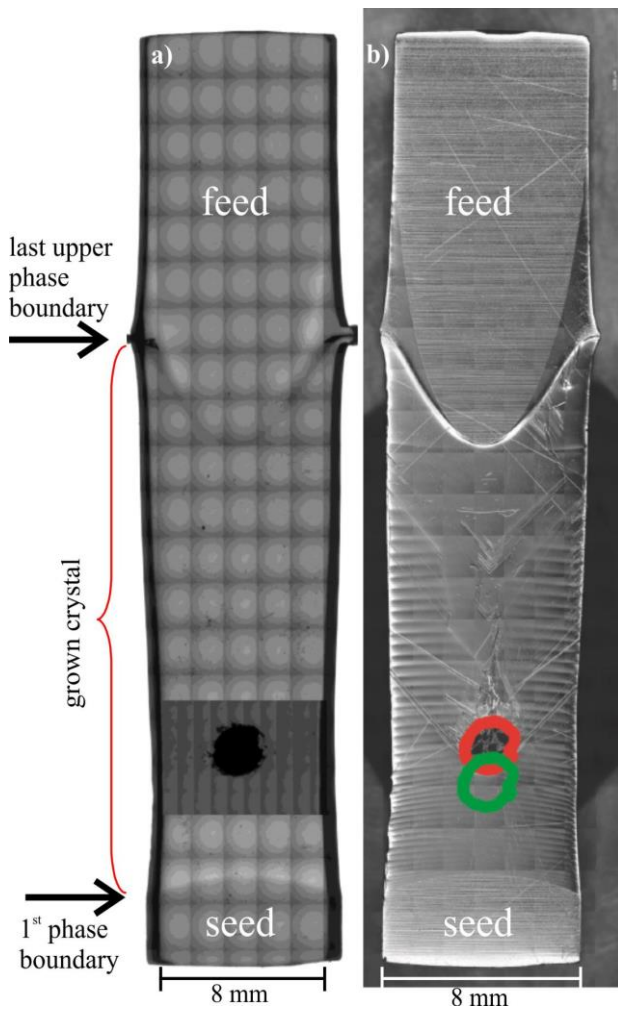
Fig. 6 a) IR transmission mapping of the µg sample, the black circle are the non-transparent SiC particles, b) Differential Interference Contrast (DIC) overview mapping of the etched µg sample, the green circle represents the original position of the SiC particles, the red circle the position where the particles were engulfed and incorporated.

size. The red triangles represent the experiments where the particles were incorporated at a certain growth velocity.

Included into these series of experiments are the growth experiments performed at NASA with static magnetic fields of different strength (up to 5 Tesla). This could be done because the results of these experiments were similar to those without external static magnetic field. The real growth velocity at the point of incorporation was determined by detailed analysis of the striations. The striations were revealed by cutting the samples parallel to the longitudinal axis into slices and subsequent surface preparation by grinding, polishing and etching. The final defect etch[18] delineates the striations,
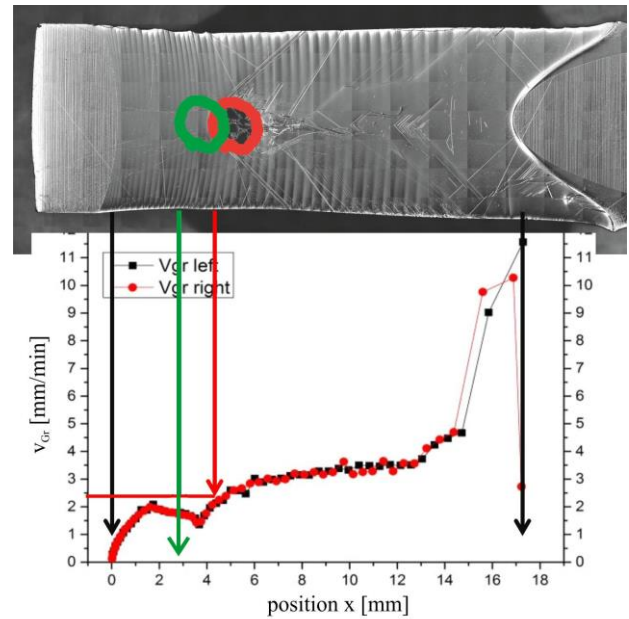
Fig. 7 Growth velocities, determined by striation analysis, correlated to crystal position in length of the µg crystal. The black arrows correspond to the first and last phase boundary, the green and red arrows mark the initial and final position of the particle slug. Vgr left and Vgr right are the growth velocities determined at the left and right crystal edge, respectively.

originating from dopant concentration oscillations due to segregation effects induced by the rotation of the sample during growth. As the rotation speed is known, the exact growth velocity can be determined this way. The exact position of the incorporated particles can be determined by using infrared (IR) transmission microscopy. The Si is IR transparent while the IR radiation is scattered at the transition Si/SiC, due to different refractive indexes. This results in black areas in the IR transmission picture at the position of the SiC particles. To achieve good contrasts, the samples are sliced and then the slices are polished on both sides.

All of the experiments were performed under conditions which theoretically should all lead to pushing the particles into the last melt zone. But it can easily be seen that the experimental results do not agree with the supposed correlation. There is a sharp border in between the bigger particles (> 30 µm) which are all incorporated, and the smaller 7 µm particles which were pushed at all applied growth velocities.

Based on these results a parameter window (indicated by the rectangle in **Fig. 5**) for the TEXUS flight was defined. It covers the most interesting growth velocities between 2 and 10 mm/min and different particle sizes with emphases at 7 and 60 µm.

3.2   Experiment under µg and 1 G Reference

As mentioned above, a mono-ellipsoid mirror furnace identical in construction to the 1 G model was used for the µg experiment on TEXUS 51. 1 G reference experiments were also done in the flight model of the furnace. The parameter window was fixed basing on the results from the 1 G experiments. **Figure 6** shows two pictures of two differently prepared slices of the processed µg sample. On the left side (**Fig. 6a**) an IR transmission mapping can be seen. The particles can be found in the center of the rod about 10 mm above the first phase boundary. The slugs stayed mostly intact as a single aggregate. The growth direction was from bottom to the top. On the right side (**Fig. 6b**) a DIC mapping of the etched slice is shown. Between the first and the very last phase boundary, striations can be seen. The distance in between the single striations changes with the change of the growth velocity and are a very precise tool for the exact determination of the growth velocity. The green circle in **Fig. 6b** represents the original position of the SiC particles before melting. The red circle, a few mm above the green one, shows the position of engulfment and incorporation of the particles. The incorporation happened at a growth velocity of 2.4 mm/min. It can also be stated that the particles stay in the center of the rod, there seems to be no force pushing them to the edges of the crystal. A phenomenon which can be observed in all crystals of this work is that polycrystalline growth starts immediately after the incorporation of the foreign phase particles. Grain boundaries originate at the position of the incorporated particles and propagate through the crystal. Vice versa, if the particles cannot be observed directly, the origin of polycrystalline growth can be assigned to incorporated SiC particles. Additionally, the striations are less visible in the polycrystalline part above the particles. The shape of the solid-liquid interface seems not to be influenced before, during and after the incorporation. **Figure 7** shows the comparison of the crystal position and the correlated growth velocities of the µg crystal, determined by striation analysis. From the diagram it can be seen that the particles were pushed about 1.5 mm from their original position until a growth velocity of 2.4 mm/min was achieved. Then the particles were engulfed and incorporated into the growing crystal. The distance of the particles to the very first phase boundary (x=0mm in diagram) is about 4.2 mm.

The µg crystal shows a strongly convex interface, which can be explained by the missing convection in the zone and therefore reduced heat transport to the center of the molten zone. It is a known effect in µg samples[15]. The strongly bent last upper interphase originates from the very high growth velocity at the end of the growth experiment. The time for melting the feed material is decreased, so the heat cannot be transported to the center parts of the zone, i.e. with increasing growth velocities the interface curvature is increased as well.

A closer look at the progress of the growth velocity in **Fig. 7** shows that the particles are incorporated during the second step of increasing the growth velocity. Due to small variations of the zone height during the FZ-growth, the growth velocity deviates in a small range. This and the inertia of the system lead to a deviation of the real growth velocities from the applied translation profile. Due to the fact that the incorporation happened during the second step of the translation speed increase, the only rise of v_{Gr} is not responsible for the particle incorporation, but it is correlated to a certain critical growth velocity v_{cr}.

Figure 8 shows the 1 G reference crystal prepared identically and investigated like the µg sample in **Fig. 6**. An IR transmission mapping is shown in **Fig. 8a** and a DIC overview of an etched slice in **Fig. 8b**.

In the IR picture no particles can be observed. Thus, the particles are located in another slice of the sample. In the DIC
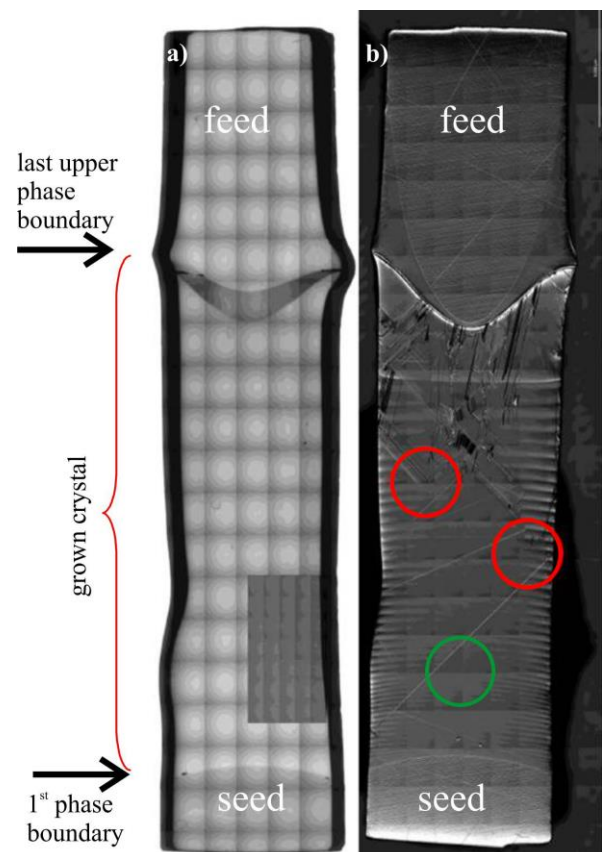
Fig. 8 a) IR transmission mapping of the 1 G sample, no SiC particles present within this slice, b) DIC overview mapping of the etched 1 G sample, The green circle represents the original position of the particle slug and the red circles represent the two distinguishable positions where particles were engulfed and incorporated, indicated by the beginning polycrystalline growth.
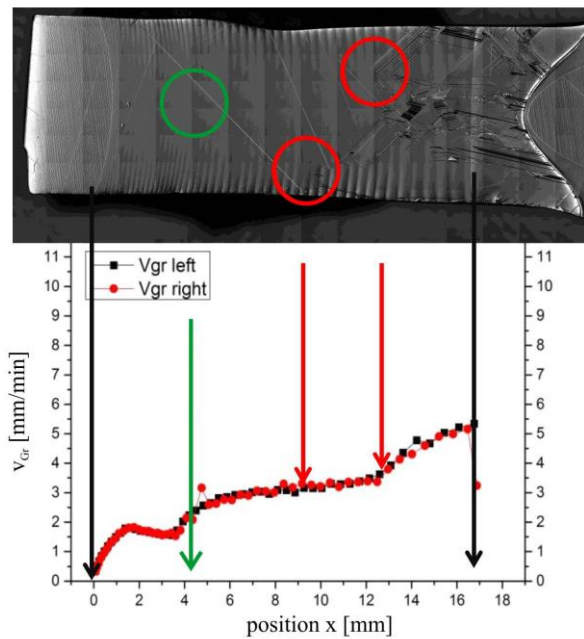
Fig. 9 Growth velocities, determined by striation analysis, correlated to crystal position in length of the 1 G crystal. The black arrows correspond to the first and last phase boundary, the green and red arrows mark the initial and final position of the particle slug. Vgr left and Vgr right are the growth velocities determined at the left and right crystal edge, respectively.

mapping it can be seen that there are 2 points within the grown region which act as origin for polycrystalline growth. As explained above, these points can be correlated to positions where particles were incorporated. **Figure 9** shows the correlated diagram with the growth velocities v_{Gr} in dependence of the position x, determined by striation analysis. The particles were incorporated at two different values for x and therefore at two different growth velocities. The first incorporation point was at 3.4 mm/min and the second one at 3.75 mm/min. It is possible that the particles split within the melt and the incorporation points might be correlated to different particle sizes, but this has to be investigated in detail. While the first particles were incorporated during a stable growth velocity section, the second part was incorporated during the increase of the translation speed from 5 to 10 mm/min. But as mentioned above, previous experiments excluded clearly that only a rise of translation speed and therefore the growth velocity alone is not indicating spontaneous particle incorporation.

Similar to the µg crystal no precipitates can be found in the 1 G reference crystal by IR microscopy. This indicates that the zone height was stable during the whole growth. Otherwise, if the zone height decreases during growth the solubility limit of C in Si is exceeded and SiC starts to precipitate. This was not the

case in these experiments, thus the chosen growth parameters were sufficient.

In contrast to the µg sample, here the particles were transported to the crystal edges likely due to buoyancy convection. This melt movement might also be responsible for the partial distribution of the particles.

4. Discussion and Conclusion

The comparison of the particle incorporation behavior during crystal growth under earth conditions (i.e. 1 G of gravity force) and µg conditions leads to the conclusion that melt convection influences the particle incorporation in a substantial way. In this work, comparable growth setups were chosen to investigate the influence of buoyancy convection. The Marangoni convection driven by free melt surfaces was suppressed by a silicon oxide layer covering the whole molten zone. In a diffusive regime without any convection, the particles are incorporated at lower growth velocities, 2.4 mm/min compared to 3.4 mm/min and 3.8 mm/min, respectively) for a convective regime. The missing lift force under µg is responsible for this effect, which is mainly due to melt convection[4]. Apparently, even small flow velocities have a significant effect, since strong static magnetic fields of up to 5T did not have a discernible influence on the incorporation. In principle there could have been thermoelectromagnetic convection[14]. However, due to a segregation coefficient ≈1 for boron in Si and a low dopant concentration it is unlikely. Typical striations indicating this effect could not be observed. External time-dependent magnetic fields, which stimulate melt convection, lead to particle pushing enhanced by the lift-force[19]. In µg the weak interface force is the only active force which counteracts the drag-force, but at some point it is too weak to avoid the particle engulfment. Additionally, the convection is also responsible for the transportation of the particles to the crystal edges, under diffusive conditions the particles stay in their original radial position. Thus, the transport is not caused by wetting effects between particle and melt.

Further investigations of the 1 G crystal should show if there was a splitting of the 7 and 60 µm particles in the melt and if the incorporation at different growth velocities was dependent on the particle size.

The Critical Growth Rate for Particle Incorporation during the Directional Solidification of Solar Silicon under Microgravity

References

1) C. Reimann, M. Trempa, J. Friedrich and G. Müller: J. Crystal Growth, **312** (2010) 1510.
2) C. Reimann, M. Trempa, T. Jung, J. Friedrich and G. Müller: J. Crystal Growth, **312** (2010) 878.
3) M. Trempa, C. Reimann, J. Friedrich and G. Müller: J. Crystal Growth, **312** (2010) 1517.
4) D.M. Stefanescu, F.R. Juretzko, B.K. Dhindaw, A. Catalina, S. Sen and P.A Curreri : Metallurgical and Materials Transactions A, **29A** (1998) 1697.
5) A.M. Zubko, V.G. Lobanov and V.V. Nikonova: Sov. Phys. Crystallogr., **18(2)** (1973) 239.
6) S.N. Omenyi and A.W. Neumann: J. Appl. Phys., **47(9)** (1976) 3956.
7) Y M. Youssef, R.J. Dashwood and P.D. Lee: Composites, Part A, **36** (2005) 747.
8) S. Sen, F. Juretzko, D.M. Stefanescu, B.K. Dhindaw and P.A. Curreri: J. Crystal Growth, **204** (1999) 238.
9) S. Mukherjee, M.A.R. Sharif and D.M. Stefanescu: Metallurgical and Materials Transactions A, **35(2)** (2004) 623.
10) A.A. Chernov, D.E. Temkin and A.M. Mel'nikova: Sov. Phys. Crystallography, **21** (1976) 369.
11) A.A. Chernov, D.E. Temkin and A.M. Mel'nikova: Sov. Phys. Crystallography, **22** (1977) 656.
12) A.K. Søiland: Silicon for Solar Cells, PhD Thesis Norwegian University of Science and Technology (2004).
13) D.M. Stefanescu, B.K. Dhindaw, S.A. Kacar and A. Moitra: Metallurgical Transactions A, **19A** (1988) 2847.
14) A. Cröll, F.R. Szofran, P. Dold, K.W. Benz and S.L. Lehoczky: J. Crystal Growth, **183** (1998) 554.
15) A. Cröll, W. Müller-Sebert, K.W. Benz and R. Nitsche: Microgravity Sci. Technol., **III/4** (1991) 204.
16) A. Eyer, A. Cröll and R. Nitsche: J. Crystal Growth, **71** (1985) 173.
17) A. Cröll, W. Müller and R. Nitsche: J. Crystal Growth, **79** (1986) 65.
18) M. Wright Jenkins: J. Electrochem. Soc., **124** (1977) 757.
19) C. M. Winkler and S. L. Rani: Powder Technology, **190** (2012) 310.